



## Agent-based modelling of glucose transport

Rolina D. van Gaalen and Mikko Karttunen

Manuscript received on November 6, 2008 / accepted on December 5, 2008

### ABSTRACT

A constant supply of glucose is vital for life. Excessive and insufficient amounts can be detrimental to the health of the cell and leads to a variety of complications in the long run. However, due to the polarized nature of glucose molecules, a family of glucose transporters are required for transport across the cell's plasma membrane. In this paper, the glucose transporter protein GLUT1 is studied using two modelling methods: a simple system of differential equations and an object oriented agent-based model. The latter approach incorporates elements of biology and communication between components into the system, yet remains relatively easy to implement. Furthermore, it yields results which are in agreement with both experimental observations and the qualitative observations of more complex mathematical models of other glucose transporters.

**Keywords:** ordinary differential equations, pi calculus, SPiM, glucose transport, GLUT1, stochastic processes, agent-based modelling.

## 1 INTRODUCTION

As the most abundant organic molecule in the biosphere [1], glucose is the primary energy source in the animal kingdom [1]. All living eukaryotic cells rely heavily on a consistent supply of glucose obtained from the diet and have developed multiple mechanisms for its synthesis, transport, and storage. Finely tuned mammalian regulatory systems ensure that glucose homeostasis is maintained under a wide array of varying conditions. Under normal circumstances, the glucose concentration in the plasma after a meal can reach levels of 7 to 8 mmol/L, while during a time of fasting it can drop to 4 to 5 mmol/L [2, 3]. In an effort to maintain a desirable blood glucose level within this range, its concentration is carefully regulated by a system of hormones and cells, the most notable of which is insulin. High insulin concentrations, caused by high glucose concentrations, promote glucose storage as glycogen in muscle and liver cells and as lipids in fat and liver cells. When glucose levels become too low, insulin levels decrease to 5 to 20% of what is measured after a meal [4]. As a result, the liver and, to a lesser degree, the kidneys release glucose into the blood. Serious consequences arise when the blood glucose concentration balance is not preserved since brain cells and other cells require a consistent supply of glucose. High glucose levels lead to damaged eyes, kidneys, nerves, and/or heart when left untreated for a prolonged period of time. On the other hand, when insufficient amounts of glucose are transported into the cells, they do not get enough energy and starve resulting in seizures, coma, and death [2, 4].

Since glucose is a hydrophilic molecule, it cannot simply permeate the cell membrane and diffuse into the cell. Instead, it is transported down its concentration gradient by means of a family of twelve passive facilitated glucose transporters (GLUT) and one  $H^+$ -coupled myo-inositol transporter (HMIT) while being transported against its concentration gradient by up to six active  $Na^+$ -dependent glucose transporters (SGLT) [5]. The transporters have various roles in different bodily tissues and fluids [2]. The characteristics of the passive transporters, the GLUTs and HMIT, are summarized in Table 1.

Glucose transporter deficiencies have been implicated in a number of diseases and disorders. For recent reviews, see Refs. [6, 7, 8]. Cancer cells, for example, are known to have accelerated metabolism, which requires an increase in glucose uptake. Since transport is limited by the availability of transporters, this increase of glucose uptake in malignant cells has been associated with an increased expression of glucose transporter proteins. Evidence suggests that both GLUT1 and GLUT3 play an essen-

tial role in cancer progression [9, 10]. Determining the transport properties and mechanisms, and subsequently targeting the GLUT isoforms involved, is therefore a potential method for treating cancer [10]. In addition, an unstimulated GLUT4 protein, the insulin-dependent glucose transporter found in the heart, skeletal muscle, and adipose tissue, has been linked to type 2 diabetes [11]. Furthermore, recent research has revealed that a deficiency in glucose transporters in the brain is a rare, but preventable cause of mental retardation [12]. Hence, the importance of a thorough understanding of glucose transporter deficiencies is apparent and begins with a careful study into the mechanisms surrounding the transportation of glucose into the cells.

Much has been done to study glucose transporters from a biological perspective [13]. However, biological systems involve more than the structures of which they are comprised: information storage, processing, and execution occur at distinct levels of organization [19]. Complex organizations of processes and signalling paths must therefore be taken into consideration: a cell's genome houses long-term information storage, proteins are crucial for short-term information storage and processing, and metabolites influence information retrieval [19]. In order to understand biology at the systems level, it is imperative that the relations between structure and dynamics of the systems be examined, rather than just the characteristics of isolated cells or organisms alone [20]. Models incorporating both the biology and the intercommunication have significant potential to greatly improve the understanding of these transporter proteins, but have unfortunately been lacking.

In this paper, we analyze a model of GLUT1 [21] using a simple system of differential equations and a new agent-based method using the Stochastic Pi Machine (SPiM) [22, 23]. While the incorporation of the aforementioned signalling pathway features into the system of differential equations is not a trivial exercise – requiring the explicit inclusion of various rate constant dependencies [24] – the SPiM approach simply and automatically accounts for these intercommunication components in an intuitive way. We present these two GLUT1 models in Section 2 and the results thereof in Section 3. In Section 4, we provide a discussion and a comparison with the more complex models to which we have thus far alluded.

## 2 THE MODELS

Glucose transporters allow for the movement of glucose across the plasma membrane either into or out of the cell. Four steps have been shown to be involved [25]:

1. **Binding:** Glucose binds to the empty protein on either face of the membrane.
2. **Transport:** The protein undergoes a conformational change which closes the one binding site and exposes the other.
3. **Dissociation:** Glucose dissociates from the protein.
4. **Recovery:** The empty GLUT1 reverts to its initial state.

In order to model the behaviour of a glucose transporter, a system of four transporter states has been proposed in [21] which correspond to the four steps presented above. Systems comprised of four and six states have been presented in the literature [26, 27, 24, 28]. However, the six-state models, which were used to model  $\text{Na}^+$ /glucose transporters (SGLT), have been shown to produce qualitatively similar predictions as four-state models [28]. For the purposes of this paper, we will use the four-state approach.

The states are defined as follows. In state one (S1), the empty binding site of the protein is exposed to the exterior of the cell. As soon as a glucose molecule binds to the exposed site, the transporter makes a transition to state two (S2). In state three (S3), the protein's binding site, bound with a glucose molecule, faces the interior of the cell. When the glucose molecule is released into the cytoplasm of the cell, GLUT1 is in state four (S4). The cycle can then repeat if an S4 GLUT1 transforms into an S1. Moreover, all of the aforementioned processes are reversible.

The following notation is used throughout this paper. Let each  $y_i$  be defined as the proportion of glucose transporters in state  $i$ . Clearly,

$$y_1, y_2, y_3, y_4 \geq 0 \quad (1)$$

and

$$y_1 + y_2 + y_3 + y_4 = 1. \quad (2)$$

**Table 1** – Subtypes of GLUT proteins.

Designation	Tissue expression	Special features
GLUT1	red blood cells [13]; erythrocytes and endothelial cells lining blood vessels of brain [2]	ubiquitously expressed and transports glucose into most cells; plays essential role when glucose levels are low, also in cases of hypoglycemia [4]
GLUT2	liver, intestine, kidney, and pancreatic $\beta$ cells [13]	functions as part of glucose sensor system in $\beta$ cells [2]; transports glucose out of $\beta$ cells and into blood stream [3]
GLUT3	brain and nerve tissue (neurons); placenta, kidney, heart, and liver [13]	GLUT1, GLUT2, and GLUT3 proteins account for $\approx 80\%$ of non-insulin dependent glucose uptake of body [3]. GLUT1 and GLUT3 allow glucose to cross blood-brain barrier and enter neurons [2].
GLUT4	heart, skeletal muscle, and adipose tissue [14]	stimulated by insulin [3]; sequestered inside a cell's special storage vesicles until stimulated to translocate to plasma membrane [14]
GLUT5	intestine, brain, muscle, adipose tissue, and testis [13]	transports fructose [2]
GLUT6	brain and leukocytes [15]	
GLUT7	liver; hepatocytes and other gluconeogenic tissues [16]	transports glucose across endoplasmic reticulum membrane [16]
GLUT8	testis, blastocysts, brain, muscle, and adipocytes [15]	$\approx 44.5\%$ identical with GLUT5 [9]
GLUT9	kidney and liver [15]; also detected in placenta, lung, blood leukocytes, heart, and skeletal muscle [17]	$\approx 31\%$ identical with GLUT3 [9]
GLUT10	liver and pancreas [14, 15]	$\approx 30\text{-}35\%$ identical with GLUT3 and GLUT8
GLUT11	heart and skeletal muscle [14, 15]	$\approx 41\%$ identical with GLUT5
GLUT12	skeletal muscle, adipose tissue, and small intestine [14]	$\approx 29\%$ identical with GLUT4 and $40\%$ with GLUT10
HMIT	brain [18]	$\approx 38\%$ identical with GLUT8

Furthermore, let rate  $k_{mn}$  denote a transporter that switches from state  $m$  to state  $n$ . Let  $[G]_{in}$  denote the intracellular glucose concentration and  $[G]_{out}$  denote the extracellular glucose concentration.

## 2.1 Transporter classes and model parameters

We further describe the four states of the model as follows (a summary of which can be found in Table 2):

**Table 2** – A summary of the rate constants for state transitions.

Forward process	Rate	Reverse process	Rate
S1-S2	$k_{12}[G]_{out}y_1$	S2-S1	$k_{21}y_2$
S2-S3	$k_{23}y_2$	S3-S2	$k_{32}y_3$
S3-S4	$k_{34}y_3$	S4-S3	$k_{43}[G]_{in}y_4$
S4-S1	$k_{41}y_4$	S1-S4	$k_{14}y_1$

- State 1:** Transporters enter S1 from two configurations: from S2 at rate  $k_{21}y_2$  and from S4 at rate  $k_{41}y_4$ . Transporters in this state can also transform to S4 at rate  $k_{14}y_1$  and S2 at rate  $k_{12}[G]_{out}y_1$ .
- State 2:** Transporters enter S2 from S1 at rate  $k_{12}[G]_{out}y_1$  and from S3 at rate  $k_{32}y_3$ . S2 transporters transition to S1 at rate  $k_{21}y_2$  and to S3 at rate  $k_{23}y_2$ .
- State 3:** Transporters enter S3 from S2 at rate  $k_{23}y_2$  and from S4 at rate  $k_{43}[G]_{in}y_4$ . In turn, transporters in S3 can transform to S4 at rate  $k_{34}y_3$  and S2 at rate  $k_{32}y_3$ .
- State 4:** Transporters enter S4 from S3 at rate  $k_{34}y_3$  and S1 at rate  $k_{14}y_1$ , while they leave the state to S3 at rate  $k_{43}y_4$  and to S1 at rate  $k_{41}y_4$ .

We set

$$\begin{aligned}
 [G]_{in} &= \frac{N_{in}}{N_A V_{cell}} \\
 &= \frac{N_{in}}{6.023 \times 10^{23} \times 1.0 \times 10^{-17}} \\
 &= 1.6603 \times 10^{-7} \times N_{in}
 \end{aligned} \tag{3}$$

where  $N_A$  is Avogadro's number ( $6.023 \times 10^{23}$  molecules/mol),  $V_{cell}$  is the volume of the cell ( $1.0 \times 10^{-17}$  L), and

$$N_{in}(t) = N_{in}(t - 1) + N_t(k_{34}t y_2 - k_{43}[G]_{in}t y_3) \tag{4}$$

is the number of glucose molecules inside the cell at time  $t$ . Note that  $N_t$  is the number of glucose transporters taken into consideration in this simulation. The approximate volume of a cell

is  $1.0 \times 10^{-13}$  L [29] and the number of GLUT1 transporters in a given cell is  $1.2 \times 10^8$ . To keep this ratio the same, but to decrease the number of transporters involved in the simulation, a cell volume of  $1.0 \times 10^{-17}$  L and 10000 GLUT1 proteins are used. Moreover, we let  $[G]_{out}$  be a free parameter and let  $\Delta t = 0.0001$  min.

## 2.2 The system of differential equations model

As the basic system and reference, we used the following model [21] for GLUT1

$$\frac{dy_1}{dt} = -k_{12}[G]_{out}y_1 + k_{21}y_2 + k_{41}y_4 - k_{14}y_1 \tag{5}$$

$$\frac{dy_2}{dt} = k_{12}[G]_{out}y_1 - k_{23}y_2 - k_{21}y_2 + k_{32}y_3 \tag{6}$$

$$\frac{dy_3}{dt} = k_{23}y_2 - k_{32}y_3 - k_{34}y_3 + k_{43}[G]_{in}y_4 \tag{7}$$

$$\frac{dy_4}{dt} = k_{14}y_1 + k_{34}y_3 - k_{43}[G]_{in}y_4 - k_{41}y_4. \tag{8}$$

where constraints (1) and (2) are satisfied. Substituting the constraints into the above gives [21]

$$\begin{aligned}
 \frac{dy_1}{dt} &= (-k_{12}[G]_{out} - k_{41} - k_{14})y_1 \\
 &\quad + (k_{21} - k_{41})y_2 - k_{41}y_3 + k_{41}
 \end{aligned} \tag{9}$$

$$\frac{dy_2}{dt} = k_{12}[G]_{out}y_1 - k_{23}y_2 - k_{21}y_2 + k_{32}y_3 \tag{10}$$

$$\begin{aligned}
 \frac{dy_3}{dt} &= -k_{43}[G]_{in}y_1 + (k_{23} - k_{43}[G]_{in})y_2 \\
 &\quad - (k_{32} + k_{43}[G]_{in} + k_{34})y_3 + k_{43}[G]_{in}
 \end{aligned} \tag{11}$$

$$y_4 = 1 - y_1 - y_2 - y_3 \tag{12}$$

where constraint (1) is satisfied [21]. This system of equations was solved using a fourth order Runge-Kutta method. The results are presented in Section 3.

## 2.3 The Stochastic Pi Machine model

As an alternative approach, we consider an agent-based method (ABM) for modelling GLUT1. This technique considers a collection of decision-making, rule-following, adaptable entities called agents. Execution of such systems occurs simply by simulating these aforementioned, potentially complex, nonlinear, or path-dependent, relationships [30, 31]. We use the Stochastic Pi Machine (SPiM) to implement this method [22, 23, 32].

**Table 3** – Summary of the parameter estimates.

Parameter	Estimate	Description	Reference
$k_{12}$	$2.4 \text{ mM}^{-1} \text{ min}^{-1}$	Rate at which extracellular glucose binds with a transporter	[21]
$k_{14}$	$1000.0 \text{ min}^{-1}$	Rate at which a free transporter changes state	[21]
$k_{21}$	$42.0 \text{ min}^{-1}$	Rate at which glucose is released outside the cell	[21]
$k_{23}$	$1000.0 \text{ min}^{-1}$	Rate at which the bounded transporter changes state	[21]
$k_{32}$	$1000.0 \text{ min}^{-1}$	Rate at which the bounded transporter changes state	[21]
$k_{34}$	$42.0 \text{ min}^{-1}$	Rate at which glucose is released inside the cell	[21]
$k_{41}$	$1000.0 \text{ min}^{-1}$	Rate at which a free transporter changes state	[21]
$k_{43}$	$2.4 \text{ mM}^{-1} \text{ min}^{-1}$	Rate at which intracellular glucose binds with a transporter	[21]
$[G]_{\text{in}}$	$(1.66 \cdot 10^{-7} N_{\text{in}}) \text{ mol/L}$	Intracellular glucose concentration	
$[G]_{\text{out}}$	variable	Extracellular glucose concentration	
$\Delta t$	0.0001 min		

Whereas mathematical modelling techniques involving differential equations require the entire set of equations to be manually updated when a small part of the model changes, the process calculi approach employed by SPiM does not. Instead, the compositional features of SPiM allow one to understand, model, analyze, and simulate complex systems by breaking them up into simpler subsystems or processes. There are three significant advantages: (1) the network structure is allowed to change as a result of interaction, (2) various complex systems may be modelled independently and later combined to yield a broader picture, and (3) modular and hierarchal structure may be incorporated into the system. Moreover, in order to facilitate the analysis of a pathway, an appropriate model would incorporate information of its molecular, biochemical, and dynamic aspects into the model. Via synchronized pair-wise communication on complementary channels, process calculus enables independent agents to interact with and modify each other. In lieu of modifying shared variables, process calculus represents interactions between agents as communication via channels.

Using the model for GLUT1 as an example, we provide a brief description of the SPiM code used here. See Figure 1 for the flow chart. The first of the four main parts is the directive section wherein the general information of the simulation is stored: the duration, the number of increments, and the “of interest” data points are noted here.

The second part defines the variables of the code: the channels, delays, and other variables. In this section, we specifically model the behaviour of the GLUT1 protein by breaking it up into two processes that run simultaneously while utilizing six complementary channels and two delays. See Figure 1.

The third partition is where the action takes place: molecules and their respective domains are treated as processes, complementary structural and chemical determinants are modelled using communication channels, and chemical interactions and the resulting system modifications are modelled as communication and channel transmissions. Channels are specified to either send (with an ‘!’) or receive communication (with a ‘?’). See Figure 1. Importantly, in this case, we also ensure that the rate of transporters changing from S4 to S3 is dependent upon the intracellular glucose concentration by including a self loop:  $\text{Glucose\_In} - \text{Glucose\_In}$ .

The final section executes the code and specifies the number of molecules involved in the entire procedure.

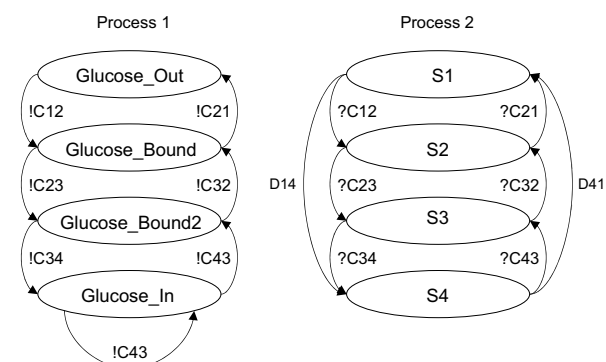


**Figure 1** – A graphical depiction of the two process used to model GLUT1 in SPiM. The path of the glucose molecule is depicted on the left, while the transformation of the transporters between states is shown on the right. The symbols !C and ?C are used to denote complimentary channels. Paths commencing with D denote delays. For example: The transition from S1 to S2 is dependent upon the presence of a glucose molecule. This dependency is modelled using a complimentary channel. On the other hand, the transition from S1 to S4 is independent and therefore we assign a delay to this path.

### 3 RESULTS

Glucose transport into the cell via GLUT1 was modelled using both a system of differential equations and object-oriented, stochastic pi calculus approach. Simulations were run and results were obtained for three extracellular glucose concentration levels: 1.5 mM, 30.0 mM, and 700.0 mM.

Results for intracellular glucose concentration levels are presented in Figure 2. In Figure 2a, it may be observed that the results are relatively similar for both models. Although the features are more pronounced in the SPiM simulations, both plots exhibit a steady increase in glucose transportation rates until about 0.2 minutes at which point the rate of uptake decreases slightly. However, as extracellular glucose concentration levels rise, so does the divergence between test results for the two modelling techniques. By 0.3 minutes, the intracellular glucose concentration levels for  $[G]_{out} = 30.0$  mM (Fig. 2b) and  $[G]_{out} = 700.0$  mM (Fig. 2c) differ between the tests by factors of about 8 and 18, respectively.

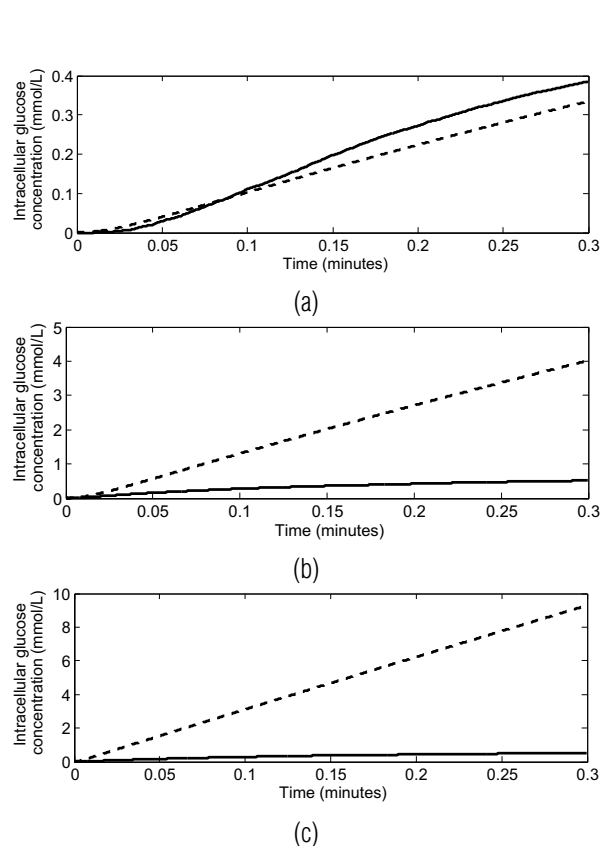


**Figure 2** – The intracellular glucose concentration with respect to time for the SPiM model and the system of differential equations 9, 10, and 11. The solid line represents the SPiM simulations and the dashed line represents the system of differential equations outcome. (a)  $[G]_{out} = 1.5$  mmol/L, (b)  $[G]_{out} = 30.0$  mmol/L, and (c)  $[G]_{out} = 700.0$  mmol/L.

Moreover, disparities between the proportion of transporters in each state are significant. For example, in comparing Figures 3a and 3b, the most obvious divergence is observed in the trends of state one and state four. While they remain at similar levels in Figure 3a, the trends head in opposite directions in Figure 3b. This discrepancy is also displayed in the  $[G]_{out} = 30.0$  mM and  $[G]_{out} = 700.0$  mM simulations. Qualitatively interesting trends may be observed when comparing the plots of states two and three for all simulations (Figs. 3b, 4b, and 5b). The reasons behind these differences will be discussed in Section 4.

It is further important to note that although 0.5–30 mM is close to the normal 4–7 mM physiological extracellular glucose concentrations, no saturation effects are detected in the results of the system of differential equations. See Figure 6a. In fact, convergence is only detected when the extracellular glucose concentration reaches levels of 700.0 mM. In contrast, results obtained from the SPiM simulations show that convergence is detected at a much lower extracellular glucose concentration (Fig. 6b).

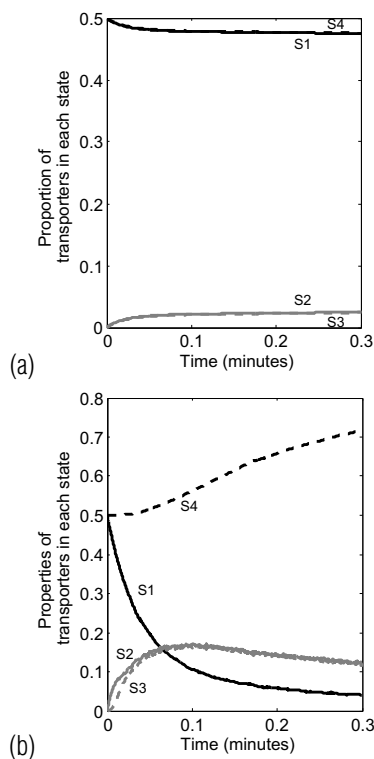


**Figure 3** –  $[G]_{out} = 1.5$  mmol/L. The proportion of transporters in each state with respect to time for (a) the system of differential equations 9, 10, and 11 and (b) SPiM simulation model. The solid black line represents the proportion of empty transporters facing the exterior of the cell, the solid grey line represents the proportion of transporters bound with glucose facing the exterior of the cell, the dashed grey line represents the proportion of transporters bound with glucose facing the interior of the cell, and the dashed black line represents the proportion of transporters facing the interior of the cell.

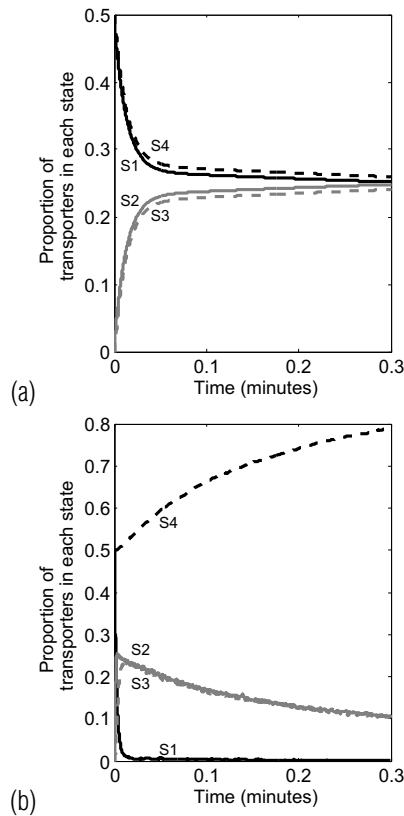


**Figure 4** –  $[G]_{\text{out}} = 30.0$  mmol/L. The proportion of transporters in each state with respect to time for (a) the system of differential equations 9, 10, and 11 and (b) SPiM simulation model. The solid black line represents the proportion of empty transporters facing the exterior of the cell, the solid grey line represents the proportion of transporters bound with glucose facing the exterior of the cell, the dashed grey line represents the proportion of transporters bound with glucose facing the interior of the cell, and the dashed black line represents the proportion of transporters facing the interior of the cell.

#### 4 DISCUSSION

Our SPiM results, most notably Figures 4b and 5b, are qualitatively similar to those found from the six-state differential equations model of  $\text{Na}^+$ /glucose cotransporters presented in [24]. In particular, the divergence of transporter states one and four, also a feature of the Parent *et al.* paper, is quite different from what is observed from the simpler differential equations model used in this paper. Therefore, an adjustment to equations (5)–(8) must be made as was done in [24]: the inclusion of exponential terms in rates  $k_{\text{mn}}$ . While this modification would likely yield more promising results (not done here), the complexity of the system increases. The benefits of an agent-based model, as was discussed in Section 2, should be clear: intercommunication and signalling paths result in more reasonable results without over complicating the system. In addition, extra features could be easily added as new processes.

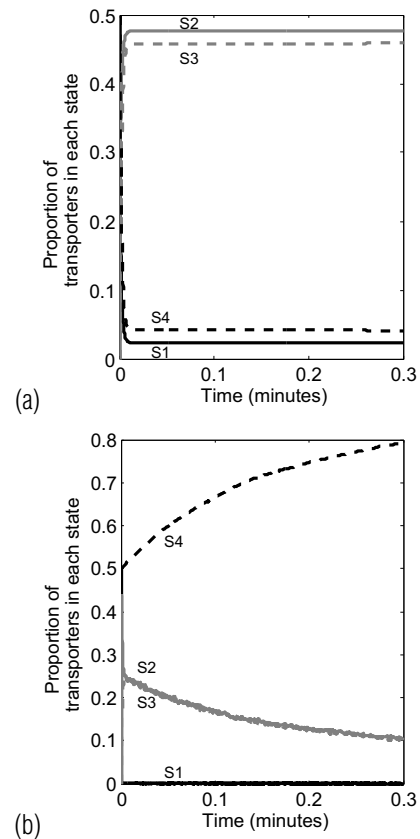


**Figure 5** –  $[G]_{\text{out}} = 700.0$  mmol/L. The proportion of transporters in each state with respect to time for (a) the system of differential equations 9, 10, and 11 and (b) SPiM simulation model. The solid black line represents the proportion of empty transporters facing the exterior of the cell, the solid grey line represents the proportion of transporters bound with glucose facing the exterior of the cell, the dashed grey line represents the proportion of transporters bound with glucose facing the interior of the cell, and the dashed black line represents the proportion of transporters facing the interior of the cell.

Furthermore, the lower level of intracellular glucose concentration convergence of the SPiM results, and the corresponding lower levels of extracellular glucose concentration at which this occurred, was more realistic than those of the system of differential equations. These results are in reasonable agreement with experiments: the mean level of intracellular glucose concentration in muscle cells has been shown to be  $0.11 \pm 0.46$  mM in non-diabetic individuals [33].

In conclusion, the agent-based modelling technique employed by SPiM is simple and efficient: adjustments to the manner in which SPiM implements biological models are relatively undemanding and intuitive. Moreover, the notions behind SPiM are relevant. In particular, the fact that complex systems can be divided into smaller parts which can later be combined is applicable in many areas of mathematical biology and beyond.

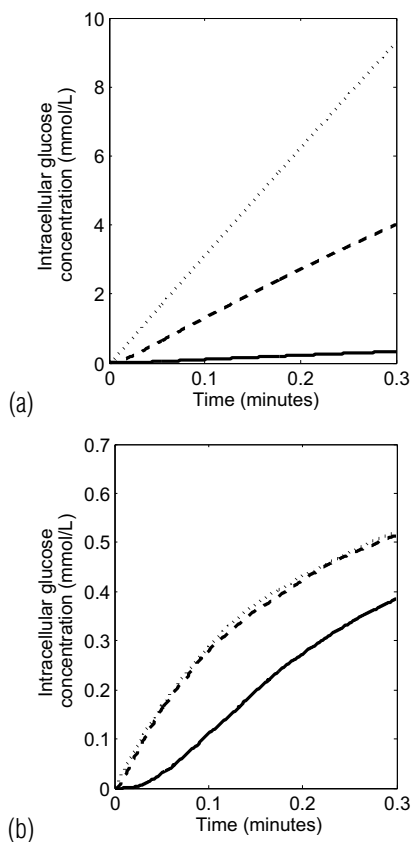


**Figure 6** – Comparing three extracellular glucose concentrations. (a) and (b). The intracellular glucose concentration with respect to time for the system of differential equations 9, 10, and 11 and the SPiM simulation model. The solid line represents an extracellular glucose concentration of 1.5 mM, the dashed line represents an extracellular glucose concentration of 30.0 mM, and the dotted line represents an extracellular glucose concentration of 700.0 mM.

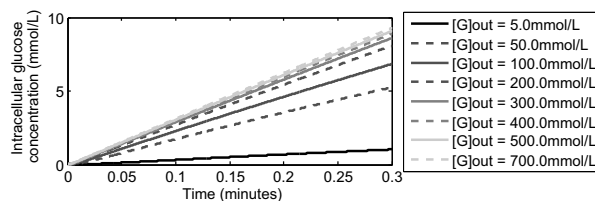


**Figure 7** – A graphical depiction of the intracellular glucose concentration with respect to time for the system of differential equations 9, 10, and 11. Note that convergence is only depicted when extracellular glucose concentration levels are at significantly higher levels than the 4–7 mM normally observed.

## ACKNOWLEDGMENTS

We thank Andrew Phillips for helpful discussions and the Laboratory of Physics of Helsinki University of Technology where part of this research was conducted. This work has been supported by Helsinki University of Technology visiting professor program (MK) and NSERC of Canada (MK). Computational resources from SharcNet ([www.sharcnet.ca](http://www.sharcnet.ca)) are gratefully acknowledged.

## REFERENCES

- [1] TETAUD E, BARRETT MP, BRINGAUD F & BALTZ T. 1997. *Biochemical Journal*, 325: 569–580.
- [2] WATSON RT, KANZAKI M & PESSIN JE. 2004. *Endocrine Reviews*, 25: 177–204.
- [3] ORBAN JC, DEROCHE D & ICHAI C. 2006. *Annales Françaises d'Anesthésie et de Réanimation*, 25: 275–279.
- [4] KUMAR S & eds. 2005. *Insulin Resistance: Insulin action and its disturbances in disease*, 63–78. John Wiley & Sons Ltd.
- [5] WOOD IS & TRAYHURN P. 2003. *British Journal of Nutrition*, 89: 3–9 January.
- [6] QUTUB AA & HUNT CA. 2005. *Brain Research Reviews*, 49: 595–617.
- [7] OBY E & JANIGRO D. 2006. *Epilepsia*, 47: 1761–1774.
- [8] KLEPPER J & LEIENDECKER B. 2007. *Developmental Medicine & Child Neurology*, 49: 707–716.
- [9] PHAY J, HUSSAIN H & MOLEY J. 2000. *Surgery*, 128: 946–951.
- [10] MACHEDA ML, ROGERS S & BEST JD. 2005. *Journal of Cellular Physiology*, 202: 654–662.
- [11] YANG Q, GRAHAM T, MODY N, PREITNER F, PERONI O, ZABOLOTNY J, KOTANI K, QUADRO L & KAHN B. 2005. *Nature*, 436: 356–362.
- [12] GORDON N & NEWTON RW. 2003. *Brain and Development*, 27: 477–480.
- [13] GOULD G & HOLMAN G. 1993. *Biochemical Journal*, 295: 329–341.
- [14] PEREIRA LO & LANCHI AH. 2004. *Progress in Biophysics and Molecular Biology*, 84: 1–27.
- [15] JOOST H-G & THORENS B. 2001. *Molecular Membrane Biology*, 18: 247–256.
- [16] HEMAT R. 2007. *Andropathy*, 11–16. Urotext.
- [17] MOBASHERI A, DOBSON H, MASON S, CULLINGHAM F, SHAKIBAEI M, MOLEY J & MOLEY K. 2005. *Cell Biology International*, 29: 249–260.
- [18] ULDRY M, IBBERSON M, HORISBERGER J-D, CHATTON J-Y, RIEDERER B & THORENS B. 2001. *The EMBO Journal*, 20: 4467–4477.
- [19] OLTVAI ZN & BARABÁSI AL. 2002. *Science*, 298: 763.
- [20] KITANO H. 2002. *Science*, 295: 1662–1664.
- [21] MARLAND ES & KEIZER JE. 2002. In: FALL CP, MARLAND ES, WAGNER JM, TYSON JJ (Eds.) *Computational Cell Biology*, 53–76. Springer-Verlag.

- [22] PHILLIPS A & CARDELLI L. 2007. In: *Computational Methods in Systems Biology (CMSB'07)*, volume 4695, 184–199. Springer Verlag, New York.
- [23] PHILLIPS A. (in press). In: *Membrane Computing and Biologically Inspired Process Calculi*.
- [24] PARENT L, SUPPLISSON S, LOO D & WRIGHT E. 1992. *The Journal of Membrane Biology*, 125: 63–79.
- [25] VOET D, VOET J & PRATT C. 2008. *Fundamentals of Biochemistry: Life at the Molecular Level*, 3rd ed., 295–321. Wiley.
- [26] MAKI L & KEIZER J. 1995. *American Journal of Physiology*, 268: C780–C791.
- [27] BAKKER B, WALSH M, TER KUILE B, MENSONIDES F, MICHELS P, OPPERDOES F & WESTERHOFF H. 1999. *Proceedings of the National Academy of Sciences of the United States of America*, 98: 10099–10103.
- [28] LAYTON H & WEINSTEIN A. 2002. *Membrane Transport and Renal Physiology*, 65–84. Springer.
- [29] RUMSEY S. 2007. *Australian Family Physician*, 36: 571–572.
- [30] VAN DYKE PARUNAK H, SAVIT R & RIOLO R. 1998. *Multi-Agent Systems and Agent-Based Simulation*, 10–25. Springer.
- [31] MACY M & WILLER R. 2002. *Annual Review of Sociology*, 28: 143–166.
- [32] PHILLIPS A. 2006. <http://research.microsoft.com/~aphillip/spim/>.
- [33] CLINE G, PETERSEN K, KRSSAK M, SHEN J, HUNDAL R, TRAJANOSKI Z, INZUCCHI S, DRESNER A, ROTHMAN D & SHULMAN G. 1999. *The New England Journal of Medicine*, 341: 240–246.